

# Higgs-Boson Benchmarks in Agreement with CDM, EWPO and BPO

S. Heinemeyer<sup>1 a</sup>

Instituto de Fisica de Cantabria (CSIC-UC), Santander, Spain

**Abstract.** We explore ‘benchmark planes’ in the Minimal Supersymmetric Standard Model (MSSM) that are in agreement with the measured cold dark matter (CDM) density, electroweak precision observables (EWPO) and  $B$  physics observables (BPO). The  $(M_A, \tan \beta)$  planes are specified assuming that gaugino masses  $m_{1/2}$ , soft trilinear supersymmetry-breaking parameters  $A_0$  and the soft supersymmetry-breaking contributions  $m_0$  to the squark and slepton masses are universal, but not those associated with the Higgs multiplets (the NUHM framework). We discuss the prospects for probing experimentally these benchmark surfaces at the Tevatron collider, the LHC and the ILC.

**PACS.** 14.80.Cp Non-standard-model Higgs bosons – 12.60.Jv Supersymmetric models

## 1 Introduction

Some of the best prospects for probing the minimal supersymmetric extension of the Standard Model (MSSM) [1] might be offered by searches for the bosons appearing in its extended Higgs sector. Searches at the Tevatron collider are starting to encroach significantly on the options for heavier MSSM Higgs bosons, particularly at large  $\tan \beta$  [2, 3]. Studies have shown that experiments at the LHC will be able to establish the existence of an SM-like Higgs boson over all its possible mass range, and also explore many options for the heavier MSSM Higgs bosons [4, 5, 6]. On the other hand, the LHC might well be unable to distinguish between the lightest MSSM Higgs boson and an SM Higgs boson of the same mass. The ILC would have much better chances of making such a distinction [7, 8, 9, 10, 11], and might also be able to produce the other MSSM Higgs bosons if they are not too heavy. Furthermore, at least in some specific MSSM scenarios, electroweak precision observables (EWPO) may also provide interesting constraints [12, 13] on the MSSM Higgs sector.

In order to correlate the implications of searches at hadron colliders and linear colliders, it is desirable to define MSSM Higgs benchmark scenarios that are suitable for comparing and assessing the relative scopes of different search strategies, see e.g. Refs. [14, 15, 16, 17].

Since the MSSM Higgs sector is governed by the two parameters  $M_A$  (or  $M_{H^\pm}$ ) and  $\tan \beta$  at lowest order, aspects of MSSM Higgs-boson phenomenology such as current exclusion bounds and the sensitivities of future searches are usually displayed in terms of these two parameters. The other MSSM param-

eters enter via higher-order corrections, and are conventionally fixed according to certain benchmark definitions [14, 15]. The benchmark scenarios commonly used in the literature encompass a range of different possibilities for the amount of mixing between the scalar top quarks, which have significant implications for MSSM Higgs phenomenology, and also include the possibility of radiatively-induced  $\mathcal{CP}$  violation. The existing benchmark scenarios designed for the MSSM Higgs sector are formulated entirely in terms of low-scale parameters, i.e., they are not related to any particular SUSY-breaking scheme and make no provision for a possible unification of the SUSY-breaking parameters at some high mass scale, as occurs in generic supergravity and string scenarios. In applications of the existing benchmark scenarios for the MSSM Higgs sector [14, 15], one is normally concerned only with the phenomenology of the Higgs sector itself. Besides the direct searches for supersymmetric particles, other constraints arising from EWPO,  $B$ -physics observables (BPO) and the possible supersymmetric origin of the astrophysical cold dark matter (CDM) are not usually taken into account. This may be motivated by the fact that the additional constraints from EWPO, BPO and CDM can depend sensitively on soft-supersymmetry breaking parameters that otherwise have minor impacts on Higgs phenomenology. For example, the presence of small flavor-mixing terms in the MSSM Lagrangian would severely affect the predictions for the BPO while leaving Higgs phenomenology essentially unchanged (see also Ref. [16] for a discussion of this issue).

Here we review a different approach [18] and adopt specific universality assumptions about the soft SUSY-breaking parameters, restricting our analysis of the MSSM to a well-motivated subspace of manageable

<sup>a</sup> Email: Sven.Heinemeyer@cern.ch

dimensionality. The new  $(M_A, \tan\beta)$  planes are specified assuming that gaugino masses  $m_{1/2}$ , soft trilinear supersymmetry-breaking parameters  $A_0$  and the soft supersymmetry-breaking contributions  $m_0$  to the squark and slepton masses are universal, but not those associated with the Higgs multiplets (the NUHM framework) (see Ref. [18] for a list of references). Within the NUHM,  $M_A$  and  $\mu$  can be treated as free parameters for any specified values of  $m_0, m_{1/2}, A_0$  and  $\tan\beta$ , so that this scenario provides a suitable framework for studying the phenomenology of the MSSM Higgs sector. Since the low-scale parameters in this scenario are derived from a small set of input quantities in a meaningful way, it is of interest to take into account other experimental constraints.

## 2 The Benchmark planes

The NUHM offers the attractive possibility [13,18] to specify  $(M_A, \tan\beta)$  planes such that essentially the whole plane is allowed by the constraints from WMAP and other observations [19]. This is done assuming that  $R$  parity is conserved, that the lightest supersymmetric particle (LSP) is the lightest neutralino  $\tilde{\chi}_1^0$ , and that it furnishes most of the cold dark matter required [20].

The  $(M_A, \tan\beta)$  planes are defined by fixing three out of the four free parameters,  $m_{1/2}, m_0, A_0$  and  $\mu$ . The first two scenarios are realized by varying  $m_{1/2}$  so as to fulfill the CDM constraint. Roughly  $m_{1/2} \sim 1.2M_A$  has to be chosen [18]. The observables that we study do not vary significantly as  $m_{1/2}$  is varied around this value. Specifically, we use the  $m_{1/2}$  that gives the value of the cold dark matter density that is closest to the central value within the allowed range,  $0.0882 < \Omega_{\text{CDM}} h^2 < 0.1204$  [19]. The parameters of the first two scenarios, **P1** and **P2**, are given in Tab. 1. The second scenario, **P2**, has been selected with a relatively small value of  $m_0$ , since previous analyses of the CMSSM (where *all* the scalar mass parameter are assumed to unify at the GUT scale, *not* leaving  $M_A$  and  $\mu$  as free parameters) indicated that values of  $m_{1/2}$  and  $m_0$  below 1 TeV are preferred, in particular by the EWPO [21,22,13] (see also Ref. [23]).

	$m_{1/2}$	$m_0$	$A_0$	$\mu$	$\chi^2_{\text{min}}$
<b>P1</b>	$\sim \frac{9}{8}M_A$	800	0	1000	7.1
<b>P2</b>	$\sim 1.2M_A$	300	0	800	3.1
<b>P3</b>	500	1000	0	250 ... 400	7.4
<b>P4</b>	300	300	0	200 ... 350	5.6

**Table 1.** The four NUHM benchmark planes are specified by the above fixed and varying parameters, allowing  $M_A$  and  $\tan\beta$  to vary freely. All mass parameters are in GeV. The rightmost column shows the minimum  $\chi^2$  value found in each plane at the points labeled as the best fits in the plots.

The other two  $(M_A, \tan\beta)$  planes are defined with fixed values of  $m_{1/2}$  and  $m_0$ , and  $\mu$  varying within a restricted range chosen to maintain the LSP density within or below the WMAP range. The parameters of

**P3** and **P4** are given in Tab. 1. We use the  $\mu$  that gives the value of the cold dark matter density that is closest to the central value within the allowed range, see above.

A likelihood analysis of these four NUHM benchmark surfaces, including the EWPO  $M_W, \sin^2\theta_{\text{eff}}, \Gamma_Z, (g-2)_\mu$  and  $M_h$  and the BPO  $\text{BR}(b \rightarrow s\gamma), \text{BR}(B_s \rightarrow \mu^+\mu^-), \text{BR}(B_u \rightarrow \tau\nu_\tau)$  and  $\Delta M_{B_s}$  was performed recently in Ref. [13]. The lowest  $\chi^2$  value in each plane, denoted as  $\chi^2_{\text{min}}$ , is shown in the rightmost column of Tab. 1, corresponding to the points labeled as the best fits in the plots below. We display in each of the following figures the locations of these best-fit points by a (red) cross and the  $\Delta\chi^2 = 2.30$  and 4.61 contours around the best-fit points in the  $(M_A, \tan\beta)$  planes for each of these benchmark surfaces. These contours would correspond to the 68 % and 95 % C.L. contours in the  $(M_A, \tan\beta)$  planes *if* the overall likelihood distribution,  $\mathcal{L} \propto e^{-\chi^2/2}$ , were Gaussian. This is clearly only approximately true, but these contours nevertheless give interesting indications on the regions in the  $(M_A, \tan\beta)$  planes that are currently preferred.

We display in each plane the region excluded (black shaded) at the 95 % C.L. by the LEP Higgs searches in the channel  $e^+e^- \rightarrow Z^* \rightarrow Zh, H$  [24,25]. For a SM-like Higgs boson we use a bound of  $M_h > 113$  GeV. The difference from the nominal LEP mass limit allows for the estimated theoretical uncertainty in the calculation of  $M_h$  for specific values of the input MSSM parameters [26]. In the region of small  $M_A$  and large  $\tan\beta$ , where the coupling of the light  $\mathcal{CP}$ -even Higgs boson to gauge bosons is suppressed, the bound on  $M_h$  is reduced to  $M_h > 91$  GeV [25].

The evaluation of the observables in the following section has been performed using the code **FeynHiggs** [26,27,28,29]. The new benchmark planes have been included into the code. This will enable the interested reader to explore the prospects for her/his favorite experimental probe of supersymmetry in these benchmark surfaces. More details can be found in the Appendix of Ref. [18].

## 3 Phenomenological analysis

We focus here on two of the four benchmark planes, **P1** and **P3**. The other two, **P2** and **P4**, respectively, show a qualitatively similar behavior due to the same choice of fixed and varied parameters. More information about **P2** and **P4** can be found in Ref. [18].

### 3.1 Tevatron

We first consider how experiments at the Tevatron collider in the next years could probe the benchmark surfaces **P1** and **P3**. We consider one possible Tevatron signature for the MSSM Higgs sector, namely  $H/A \rightarrow \tau^+\tau^-$ , for which expectations are evaluated using the results from Ref. [30]. We see in Fig. 1 that, at the Tevatron with 2 (4, 8) fb<sup>-1</sup> of integrated and analyzed luminosity per experiment the channel  $H/A \rightarrow$

$\tau^+\tau^-$  would provide a 95% C.L. exclusion sensitivity to  $\tan\beta \sim 35(30,25)$  when  $M_A \sim 200$  GeV, and the sensitivity decreases slowly (rapidly) at smaller (larger)  $M_A$ . In the case of the benchmark surface **P1**,  $8 \text{ fb}^{-1}$  would start accessing the region with  $\Delta\chi^2 < 4.61$ . The region  $\Delta\chi^2 < 4.61$  could be accessed already with  $2 \text{ fb}^{-1}$  in case **P3**, and  $8 \text{ fb}^{-1}$  would give access to the region with  $\Delta\chi^2 < 2.30$ .

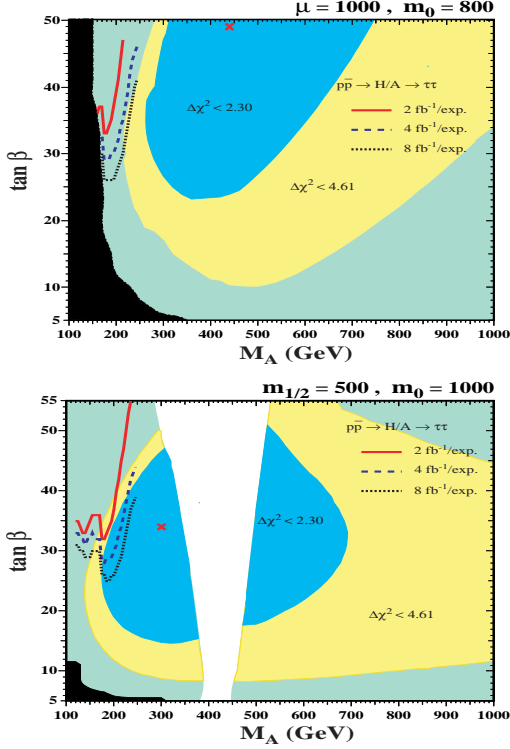


**Fig. 1.** The  $(M_A, \tan\beta)$  planes **P1** (upper) and **P3** (lower plot), displaying the expected 95% C.L. exclusion sensitivities of searches for  $H/A \rightarrow \tau^+\tau^-$  at the Tevatron collider with 2, 4, 8  $\text{fb}^{-1}$  in each of the CDF and D0 experiments.

### 3.2 LHC

Here we analyze the LHC reach for the heavy MSSM Higgs bosons. In Fig. 2 we display in the  $(M_A, \tan\beta)$  planes the 5- $\sigma$  discovery contours for  $b\bar{b} \rightarrow H/A \rightarrow \tau^+\tau^-$  at the LHC, where the  $\tau$ 's decay to jets and electrons or muons [31,32,33], based on 60 or 30  $\text{fb}^{-1}$  collected with the CMS detector. As shown in Ref. [34], the impact of the supersymmetric parameters other than  $M_A$  and  $\tan\beta$  on the discovery contours is relatively small in this channel. The discovery contours in the benchmark surfaces are therefore similar to each other and to those in the “conventional” benchmark scenarios [34].

We also show in Fig. 2 the 5- $\sigma$  contours for discovery of the  $H^\pm$  via its  $\tau^\pm\nu$  decay mode at the LHC, in the case  $M_{H^\pm} > m_t$ . The coverage is limited to  $M_A < 300$  GeV and  $\tan\beta > 30$ .

### 3.3 ILC

Finally, we show in Fig. 3 the prospective sensitivity of an ILC measurement of the  $\text{BR}(h \rightarrow b\bar{b})$  in

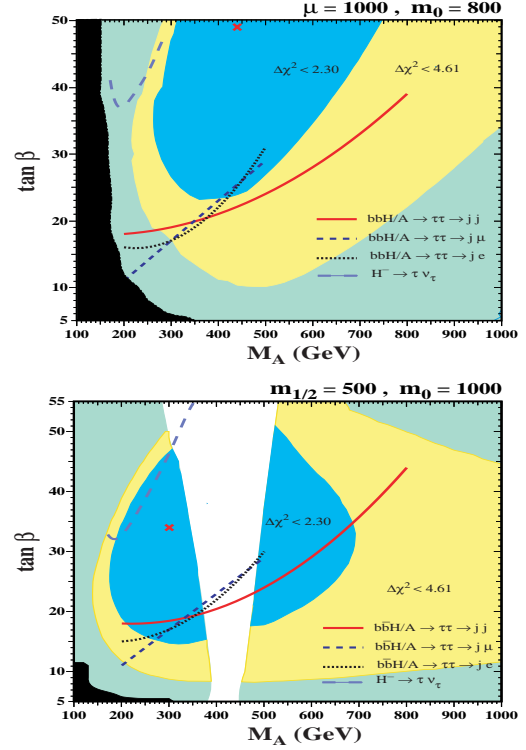


**Fig. 2.** The  $(M_A, \tan\beta)$  planes **P1** (upper) and **P3** (lower plot), displaying the 5- $\sigma$  discovery contours for  $H/A \rightarrow \tau^+\tau^-$  at the LHC with 60 or 30  $\text{fb}^{-1}$  (depending on the  $\tau$  decay channels) and for  $H^\pm \rightarrow \tau^\pm\nu$  detection in the CMS detector when  $M_{H^\pm} > m_t$ .

the two  $(M_A, \tan\beta)$  planes. The experimental precision is anticipated to be 1.5%, see Ref. [7] and references therein. We display as solid (blue) lines the contours of the +5, +3, +2, +1, 0  $\sigma$  deviations (with +2  $\sigma$  in bold) of the MSSM result from the corresponding SM result. The separations between the contours indicate how sensitively the SUSY results depend on variations of  $M_A$  and  $\tan\beta$ . Also shown in Fig. 3 via dashed (green) lines is the sensitivity to SUSY effects of the ILC measurement of the ratio of branching ratios  $\text{BR}(h \rightarrow b\bar{b})/\text{BR}(h \rightarrow WW^*)$ , see Ref. [7] and references therein. The precision measurement of the ratio  $\text{BR}(h \rightarrow b\bar{b})/\text{BR}(h \rightarrow WW^*)$  clearly provides a much higher sensitivity to SUSY effects than the measurement of  $\text{BR}(h \rightarrow b\bar{b})$  alone (see also Ref. [9]). For nearly the full planes a  $\sim \text{few } \sigma$  effect can be established at the ILC.

### Acknowledgements

We thank J. Ellis, T. Hahn, K.A. Olive, A.M. Weber and G. Weiglein for collaboration on the work presented here. Work supported in part by the European Community’s Marie-Curie Research Training Network under contract MRTN-CT-2006-035505 ‘Tools and Precision Calculations for Physics Discoveries at Colliders’.

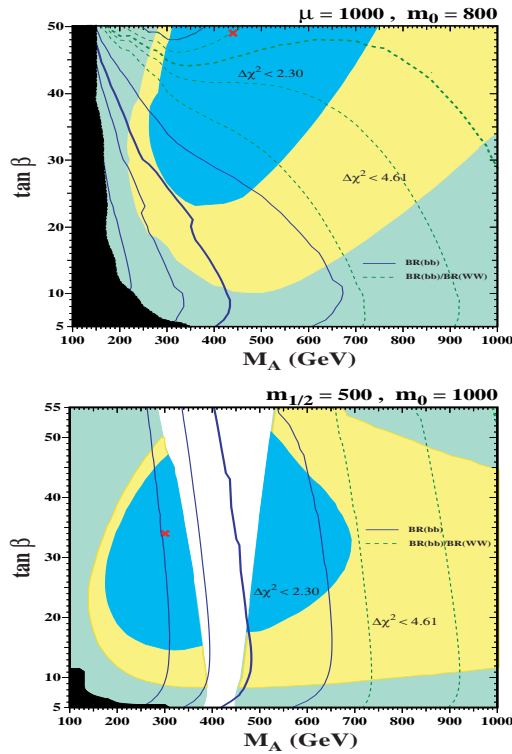


**Fig. 3.** The  $(M_A, \tan \beta)$  planes **P1** (upper) and **P3** (lower plot), displaying 5, 3, 2, 1, 0- $\sigma$  sensitivity contours (2- $\sigma$  in bold) for SUSY effects on  $\text{BR}(h \rightarrow b\bar{b})$  (solid blue lines) and  $\text{BR}(h \rightarrow b\bar{b})/\text{BR}(h \rightarrow WW^*)$  (dashed green lines) at the ILC.

## References

1. H. Nilles, *Phys. Rept.* **110** (1984) 1; H. Haber and G. Kane, *Phys. Rept.* **117** (1985) 75; R. Barbieri, *Riv. Nuovo Cim.* **11** (1988) 1.
2. CDF Collaboration, CDF note 8676, see: [www-cdf.fnal.gov/~aa/mssm\\_htt\\_1fb/note/cdf8676.pdf](http://www-cdf.fnal.gov/~aa/mssm_htt_1fb/note/cdf8676.pdf).
3. D0 Collaboration, D0 Note 5331-CONF, see: [www-d0.fnal.gov/cgi-bin/d0note?5331](http://www-d0.fnal.gov/cgi-bin/d0note?5331).
4. M. Schumacher, *Czech. J. Phys.* **54** (2004) A103; arXiv:hep-ph/0410112.
5. S. Abdullin et al., *Eur. Phys. J. C* **39S2** (2005) 41.
6. CMS Collaboration, *Physics Technical Design Report, Volume 2. CERN/LHCC 2006-021*, see: [cmsdoc.cern.ch/cms/cpt/tdr/](http://cmsdoc.cern.ch/cms/cpt/tdr/).
7. S. Heinemeyer et al., arXiv:hep-ph/0511332.
8. A. Djouadi, arXiv:hep-ph/0503173.
9. K. Desch, E. Gross, S. Heinemeyer, G. Weiglein and L. Zivkovic, *JHEP* **0409** (2004) 062 [arXiv:hep-ph/0406322].
10. J. Ellis, S. Heinemeyer, K. Olive and G. Weiglein, *JHEP* **0301** (2003) 006 [arXiv:hep-ph/0211206].
11. A. Dedes, S. Heinemeyer, S. Su and G. Weiglein, *Nucl. Phys. B* **674** (2003) 271 [arXiv:hep-ph/0302174].
12. S. Heinemeyer, W. Hollik and G. Weiglein, *Phys. Rept.* **425** (2006) 265 [arXiv:hep-ph/0412214].
13. J. Ellis, S. Heinemeyer, K. Olive, A.M. Weber and G. Weiglein, *JHEP* **0708** (2007) 083 [arXiv:0706.0652 [hep-ph]].
14. M. Carena, S. Heinemeyer, C. Wagner and G. Weiglein, *Eur. Phys. J. C* **26** (2003) 601 [arXiv:hep-ph/0202167]; *Eur. Phys. J. C* **45** (2006) 797 [arXiv:hep-ph/0511023].
15. M. Carena, J. Ellis, A. Pilaftsis and C. Wagner, *Phys. Lett. B* **495** (2000) 155 [arXiv:hep-ph/0009212].
16. B. Allanach et al., *Eur. Phys. J. C* **25** (2002) 113 [arXiv:hep-ph/0202233].
17. M. Battaglia et al., *Eur. Phys. J. C* **22** (2001) 535 [arXiv:hep-ph/0106204]; M. Battaglia et al., *Eur. Phys. J. C* **33** (2004) 273 [arXiv:hep-ph/0306219]; A. De Roeck et al., *Eur. Phys. J. C* **49** (2007) 1041 [arXiv:hep-ph/0508198].
18. J. Ellis, T. Hahn, S. Heinemeyer, K. Olive and G. Weiglein, arXiv:0709.0098 [hep-ph].
19. C. Bennett et al., *Astrophys. J. Suppl.* **148** (2003) 1 [arXiv:astro-ph/0302207]; D. Spergel et al. [WMAP Collaboration], *Astrophys. J. Suppl.* **148** (2003) 175 [arXiv:astro-ph/0302209]; D. Spergel et al. [WMAP Collaboration], *Astrophys. J. Suppl.* **170** (2007) 377 [arXiv:astro-ph/0603449].
20. H. Goldberg, *Phys. Rev. Lett.* **50** (1983) 1419; J. Ellis, J. Hagelin, D. Nanopoulos, K. Olive and M. Srednicki, *Nucl. Phys. B* **238** (1984) 453.
21. J. Ellis, S. Heinemeyer, K. Olive and G. Weiglein, *JHEP* **0502** (2005) 013 [arXiv:hep-ph/0411216].
22. J. Ellis, S. Heinemeyer, K. Olive and G. Weiglein, *JHEP* **0605** (2006) 005 [arXiv:hep-ph/0602220].
23. J. Ellis, K. Olive, Y. Santos and V. Spanos, *Phys. Rev. D* **69** (2004) 095004 [arXiv:hep-ph/0310356]; B. Allanach and C. Lester, *Phys. Rev. D* **73** (2006) 015013 [arXiv:hep-ph/0507283]; B. Allanach, *Phys. Lett. B* **635** (2006) 123 [arXiv:hep-ph/0601089]; R. de Austri, R. Trotta and L. Roszkowski, *JHEP* **0605** (2006) 002 [arXiv:hep-ph/0602028]; *JHEP* **0704** (2007) 084 [arXiv:hep-ph/0611173]; arXiv:0705.2012 [hep-ph]; B. Allanach, C. Lester and A.M. Weber, *JHEP* **0612** (2006) 065 [arXiv:hep-ph/0609295]; B. Allanach, K. Cranmer, C. Lester and A.M. Weber, arXiv:0705.0487 [hep-ph]; O. Buchmueller et al., to appear in *Phys. Lett. B*, arXiv:0707.3447 [hep-ph].
24. LEP Higgs working group, *Phys. Lett. B* **565** (2003) 61 [arXiv:hep-ex/0306033].
25. LEP Higgs working group, *Eur. Phys. J. C* **47** (2006) 547 [arXiv:hep-ex/0602042].
26. G. Degrandi, S. Heinemeyer, W. Hollik, P. Slavich and G. Weiglein, *Eur. Phys. J. C* **28** (2003) 133 [arXiv:hep-ph/0212020].
27. S. Heinemeyer, W. Hollik and G. Weiglein, *Comput. Phys. Commun.* **124** (2000) 76 [arXiv:hep-ph/9812320]; see: [www.feynhiggs.de](http://www.feynhiggs.de).
28. S. Heinemeyer, W. Hollik and G. Weiglein, *Eur. Phys. J. C* **9** (1999) 343 [arXiv:hep-ph/9812472].
29. M. Frank, T. Hahn, S. Heinemeyer, W. Hollik, H. Rzehak and G. Weiglein, *JHEP* **0702** (2007) 047 [arXiv:hep-ph/0611326].
30. CDF Collaboration, see: [www-cdf.fnal.gov/physics/projections/](http://www-cdf.fnal.gov/physics/projections/).
31. S. Gennai, A. Nikitenko and L. Wendland, CMS Note 2006/126.
32. R. Kinnunen and S. Lehti, CMS Note 2006/075.
33. A. Kalinowski, M. Konecki and D. Kotlinski, CMS Note 2006/105.
34. S. Gennai et al., to appear in *Eur. Phys. J. C*, arXiv:0704.0619 [hep-ph].